A Novel Intraoperative Force Estimation Method via Electrical Bioimpedance Sensing

Cheng, Zhuoqi; Mattos, Leonardo S.

Published in:
Advances in Service and Industrial Robotics

DOI:
10.1007/978-3-031-32606-6_25

Publication date:
2023

Document version:
Accepted manuscript

Citation for pulished version (APA):
Cheng, Z., & Mattos, L. S. (2023). A Novel Intraoperative Force Estimation Method via Electrical Bioimpedance Sensing. In T. Petrič, A. Ude, & L. Žlajpah (Eds.), *Advances in Service and Industrial Robotics: RAAD 2023* (pp. 213–220). Springer. https://doi.org/10.1007/978-3-031-32606-6_25

A Novel Intraoperative Force Estimation Method via Electrical Bioimpedance Sensing

Zhuoqi Cheng[1] and Leonardo S. Mattos[2]

[1] Maersk Mc Kinney Moller Institute, University of Southern Denmark, Odense, Denmark
zch@mmmi.sdu.dk
[2] Department of Advanced Robotics, Istituto Italiano di Tecnologia, Genova, Italy
Leonardo.DeMattos@iit.it

Abstract. During minimally invasive robotic surgery (MIRS), intraoperative force sensing on the surgical tool plays an important role to mitigate the risk of inadvertent tissue damage. This study proposes a novel method for estimating the force exerted by the surgical tool tip based on the electrical bioimpedance (EBI) of the contacting tissue. When the surgical tool is pressing on the tissue, the tissue is deformed corresponding to the exerted force. Meanwhile, the measured EBI value changes accordingly since tissue deformations change the contact area between the tool and the tissue. An ex-vivo experimental study was performed and different machine learning methods were tested for correlating the exerted force and the EBI values. The experimental results show that a Feed-forward Multi-layer Neural Network (F-MNN) can provide good results in terms of efficiency and accuracy. The exerted force on the tissue can be accurately estimated with a median error of 0.072 N and with about 7 ms testing time. In addition, the proposed method has significant advantages over other techniques since it requires little hardware modification and allows fast and seamless integration with the existing surgical robotic system.

Keywords: Force sensing · electrical bioimpedance · robot-assisted surgery.

1 Introduction

Minimally invasive robotic surgery (MIRS) has been demonstrated to significantly improve surgical outcomes, but different aspects of current systems can still be improved. One of the main issues is the perception feedback for surgeons. For most existing surgical robots, only visual information is provided. Haptic feedback is considered valuable for improving the surgical quality, but it is absent for most robotic systems. Without force feedback, surgeons were found to generally increase the average applied force on the tissue [17], tending to increase the risk of tissue damages. For example, as reported by Giannarou *et al.*[7], the allowed pressing force on brain tissue during a neurosurgery should be constrained to be less than 0.3 N. Failure to stay below this force threshold can result in an iatrogenic injury, which in turn carries a risk of disability or even death [9, 14]. In addition, the magnitude of the exerted force on liver is required to be controlled. Liver tissue can be damaged if a stress over 162.5 kPa is generated by the exerted force [16].

For restoring the pushing force feedback capability in MIRS, the most common method has been to design integrated force sensors for the surgical tools. In the study of Arata *et al.* [1], a force/torque sensor was designed and mounted in the driving units of a slave robot arm. By this means, the forces and moments acting at the surgical instrument were sensed indirectly. In another study [12], Marcus *et al.* developed a handheld robot for assisting the surgeon in handling delicate tissue by constraining the applying force on the tissue during microsurgery. In addition, a miniaturized 6-DOF force/torque sensor was developed [10]. This sensor was attached to the distal end of a forceps instrument, enabling direct measurement of forces and moments acting on it. However, the above designs require complicated and costly hardware development. As an alternative, a novel forceps with controllable constant torque has been developed [5]. Also, other researchers have proposed to estimate the exerted force by observing the tissue deformation using laparoscopic vision [7].

In this study, a new force sensing method is proposed by measuring the electrical bioimpedance (EBI) of the contacting tissue during the tool-tissue interaction. The proposed method is verified based on a bipolar robotic surgical tool which is commonly used for electrification [8]. Such tools have a pair of electrically isolated jaws which can be used as bipolar electrodes for measuring the EBI of the tissue in contact [2]. When the forceps is pushing on the soft tissue, the tip of the forceps is immersed into it. This changes the contact area between the tool tip and the tissue, which consequently changes the electric field applied on the tissue under measurement, altering the measured EBI value. Meanwhile, a corresponding reacting force is generated. This study aims to model the relationship between the exerted force and the measured EBI value, which can allow estimating the pushing force based on EBI measurements. The proposed method can be easily integrated into the readily available surgical system, requiring only small modifications to existing instruments.

2 Methodology

This study uses a hepatic MIRS scenario as an example for illustrating the proposed force sensing method. The proposed method allows setting the maximum interaction force to be 1 N to avoid damaging the liver tissue [16, 15].

As shown in Fig. 1(A), the EBI of the contacting tissue is measured continuously via two jaws of a bipolar forceps. An alternative voltage U is applied between them and the reciprocal current I is measured. According to [4], the current I can be obtained by integrating the current density J through the tissue range r.

$$|Z| = \int_{\Omega} (\frac{J}{\hat{\sigma}}) d\Omega = \frac{1}{2\pi\hat{\sigma}} (\frac{1}{r_0} - \frac{1}{r}) \tag{1}$$

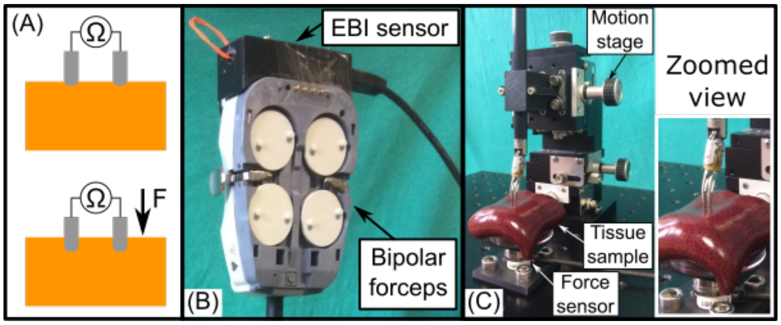

Fig. 1. (A) $|Z|$ is measured between two jaws of the forceps during its pressing on the soft tissue; (B) The EBI sensor prototype integrated to a da Vinci Maryland bipolar forceps; (C) The experimental setup for collecting both the pressing force and the EBI value simultaneously.

where r_0 is the equivalent radius of the electrode immersing in the tissue, and $\hat{\sigma}$ represents the complex conductivity of tissue. When the forceps is pressing deeper, r_0 increases gradually. In this case, the measured EBI value $|Z|$ decreases accordingly. Thus, the force estimation can be done by the correlation between the pressing force F and the EBI value of the contacting tissue $|Z|$.

3 Experimental Setup

An ex-vivo experiment was conducted for measuring the exerted force and the corresponding EBI value simultaneously. The EBI sensor designed and presented in the previous study [2] was adopted. The EBI sensor integrates a micro-controller (Atmega328P, Atmel Inc., USA) and an impedance converter (AD5933, Analog Devices Inc., USA), allowing accurate EBI measurement at multiple frequencies. A prototype was made as shown in Fig. 1(B), which could be directly mounted on a da Vinci Maryland bipolar forceps (Intuitive Surgical Inc., USA). The measured EBI values were streamed in real-time to a PC via an USB connection. In this study, five excitation frequencies (20, 40, 60, 80 and 100 kHz) were chosen and applied for the EBI measurement. The frequencies within this range were found to provide both intracellular and extracellular electrical characteristics of the tissue under measurement [13].

Fig. 1(C) shows the experimental setup for collecting both the pressing force and the EBI value simultaneously. To measure the downward force exerted from the top of the tissue by the forceps, a force sensor Nano17 (ATI Industrial Automation, Inc., USA) was used and placed beneath the tissue sample carrier. The Maryland bipolar forceps was fixed to a precision motion stage (Siskiyou Co., USA) with the EBI sensor connected to its poles. In this work, we upgraded the motion stage shown in Fig. 1(C) to a motorized version. The forceps was driven to move 8 mm downwards and then 8 mm upwards in a constant speed. Two speed settings were tested, namely 0.1 and 0.05 mm/s. During the experiment,

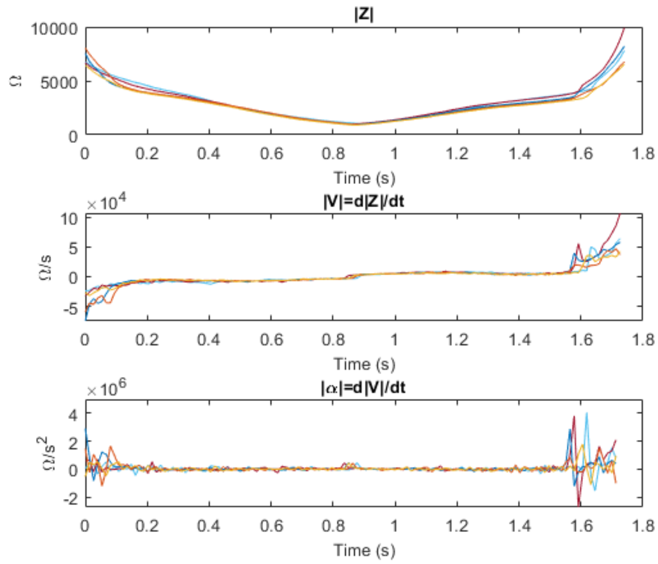

Fig. 2. Example of input EBI data: the top figure is the 5D EBI values $|Z|$, the middle figure is the 5D velocity of the EBI values $|V|$ and the bottom figure is the 5D acceleration of the EBI values $|\alpha|$. Different colours are used for representing different $|Z|$ components at 5 different excitation frequencies.

the pressing force in Z direction and the corresponding EBI values were recorded at the same time.

4 Data analysis

The aim of this procedure is to construct a regression model $f \in \mathcal{F}$ parametrized in $\Theta \in \mathbb{R}^d$ such that $\hat{F} = f(\mathtt{X}; \Theta)$ is close to the real output F. The collected time-varying input-output pairs $\mathcal{P}_t = \{\mathtt{X}_t, F_t\}$ were divided into the training dataset $\mathcal{P}_t^A$ for establishing the prediction model f and the testing datasets $\mathcal{P}_t^B$ for evaluating the performance of the model f. Considering that soft tissue is normally modelled as a spring-damper system, the velocity of the EBI values $|V|$, can play an important role for predicting F. In addition, the acceleration of the EBI values $|\alpha|$ could potentially improve the performance of the regression model, and thus it was considered for model comparison. In the following regression study, three different input components, i.e., 5D-$[|Z|]$, 10D-$[|Z|, |V|]$ or 15D-$[|Z|, |V|, |\alpha|]$, were evaluated in terms of accuracy and efficiency. The regression study was implemented in MATLAB 2018b. Fig. 2 shows the three types of inputs computed on one set of the collected data. The EBI values $|Z|$ at 5 different excitation frequencies were plotted in different colours.

Artificial Neural Network (ANN) is selected to solve the regression problem, which does not require the mathematical model of the system and has the learning capacity to fit any complex function and non-linear relationships. The following factors which could limit the performance of the model were investigated in this study, namely, the amount of neurons in the hidden layer, the number of hidden layers, and the types of ANN and the dimension of inputs. To find the best model f^*, both of the Feed-forward Neural Network (F-NN) and Cascade-forward NN (C-NN) with the back-propagation learning strategy were implemented in this work. Meanwhile, the adopted NN models were constructed with both single layer (SNN) and multi-layer (MNN) for performance comparison. The Broyden–Fletcher–Goldfarb–Shanno algorithm [11] was used to calculate the maximum or minimum gradient during the network parameters optimization. To improve the effectiveness of the ANN models, we adopted a series of optimization processing, like setting 1.05 as the increase learning rate and 6 as the maximum validation failures.

The performance of the model f was evaluated by measuring the Root Mean Square Error (RMSE) and the Pearson correlation coefficient (Corr) (Eq. 2).

$$\begin{aligned} RSME &= \sqrt{\tfrac{1}{N}\textstyle\sum_{t=1}^{N}(\hat{F}_t - F_t)^2} \\ Corr &= \tfrac{1}{N-1}\textstyle\sum_{t=1}^{N}\left(\tfrac{\hat{F}_t-\mu_{\hat{F}}}{\sigma_{\hat{F}}}\right)\left(\tfrac{F_t-\mu_F}{\sigma_F}\right) \end{aligned} \tag{2}$$

where N demotes the length of the observed force sequences F and the predicted sequences $\hat{F}$. $\mu_{\hat{F}}$ and $\sigma_{\hat{F}}$ are the average and standard deviation of $\hat{F}$, while μ_F and σ_F represent the same values of F.

5 Results

The comparison experiments were implemented with the leave-one-out strategy. In total, 26 groups of datasets were collected, half of which were collect in a pushing speed of 0.1 mm/s and the others were in a speed of 0.05 mm/s. We use 25 datasets to build the ANN-based models and a randomly selected dataset (from those acquired using 0.05 mm/s) to evaluate and compare the performance among them. Fig. 3 shows the RMSE and correlation coefficient of the four models including two MNN models (C-MNN and F-MNN) with two hidden layers and two SNN models (C-SNN and F-SNN). For the results showing in Fig. 3, both MNN models choose 20 and 10 neurons for each layer and both SNN models have 30 nodes in their hidden layer.

The comparison results of RMSE illustrate that the F-MNN is the best regression model with 10D inputs, which has the lowest RMSE (median value 0.0722 N, standard deviation 0.0078). Although all of the ANN models have similar results of Corr ($\approx$0.92) according to the tests on the 10D and 15D inputs datasets, the F-MNN model gets the most robust results with the lowest standard deviation (0.0116).

The first step of model construction proved that F-MNN with 10D inputs ($\mathtt{X} = [|Z|, |V|]$) is the best choice for mapping the EBI values to the pressing

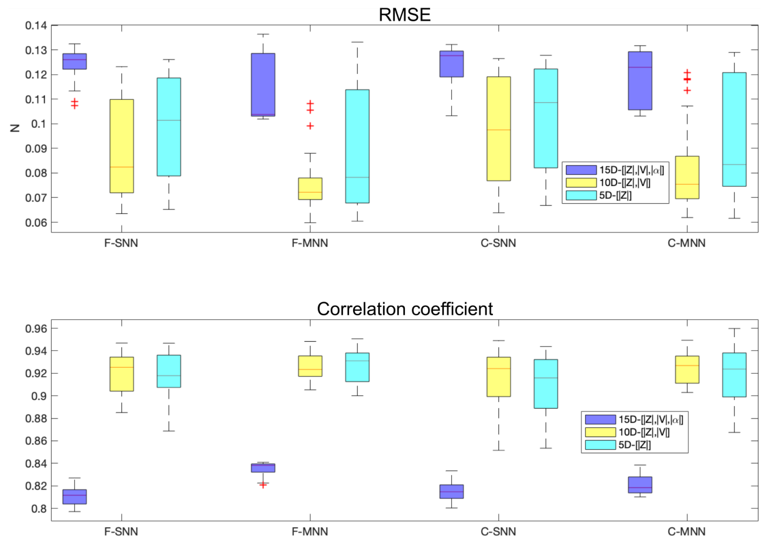

Fig. 3. The comparison results of RMSE and correlation coefficient among the four ANN-based models, i.e., F-SNN, F-MNN, C-SNN and C-MNN. For each model, it is tested by the three types of inputs with 5D (purple), 10D (yellow) and 15D (cyan).

force within the sets of tested models. Furthermore, the number of neurons in the hidden layer were tested in order to optimise the performance of ANN-based model f. Even though the results were close to each other, the F-MNN[20 10] model was found to be the best model for fast and robust computation with high accuracy.

Fig. 4 shows the predicted pressing force $\hat{F}$ and the calculated RMSE based on the F-MNN[20 10] model. The results demonstrate that the designed model can track the observed force with 10D inputs accurately. The RMSE is smaller than 0.02 N during the forceps pressing into the tissue and smaller than 0.06 N when it was pulled up.

6 Discussion and conclusion

This study proposed a new method for estimating the pushing force of surgical tool on soft tissue, aiming to incorporate force feedback onto the RMIS system with minimal hardware modifications. When the forceps presses on the tissue, the indentation of the tissue changes the contact area between the forceps and the tissue, and this is reflected on the measured EBI value. Although the electrical conductivity of bio-tissue can be compression-dependent, the compression rate in this study is generally low (about 20-30%) which corresponds to a <8% increase of $|Z|$ according to the study of Dodde *et al.* [6]. Therefore, the change of contacting area between the electrodes and the tissue during the tool-tissue interaction is considered as the main reason.

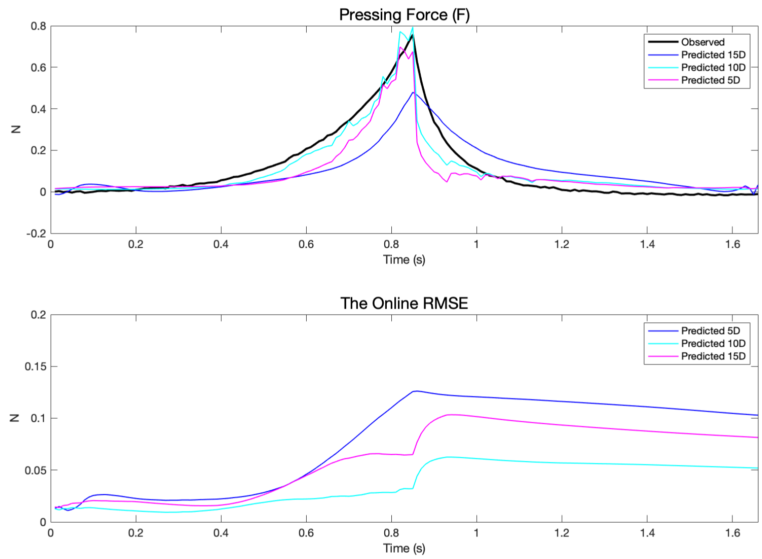

Fig. 4. An example of the comparison results of the predicted pressing forces and the online RMSE on the testing datasets with 5D, 10D and 15D inputs.

The regression model shows that the 10D model has the highest fitting accuracy. This is reasonable since the mechanical property of soft tissue can be modelled as a spring-damper system. Nevertheless, the second derivative, corresponding to $|\alpha|$, is found not contributing to F estimation. Instead, it introduces noise to the model. This may be because a constant speed of forceps movement was used in the experiment. To investigate this factor, more experiments with dynamic tool-tissue interaction will be planned in the future study.

The main limitation of the proposed method is that the trained regression model is tissue specific. Since different tissues have different electrical properties [3], it would be required to characterise each tissue of interest before implementing the proposed method. In this case, an automated tissue identification method by EBI sensing [2] can also be used. With this prior knowledge, the proposed force sensing method can be applied in a more general manner. Nevertheless, considering the current limitations regarding model dependency on tissue type and the low controllability of the contacting area between the electrode and the tissue, the proposed method may be more appropriate for surgical scenarios requiring less precision of force measurement.

References

1. Arata, J., Mitsuishi, M., Warisawa, S., Tanaka, K., Yoshizawa, T., Hashizume, M.: Development of a dexterous minimally-invasive surgical system with augmented force feedback capability. In: 2005 IEEE/RSJ International Conference on Intelligent Robots and Systems. pp. 3207–3212. IEEE (2005)

2. Cheng, Z., Dall'Alba, D., Foti, S., Mariani, A., Chupin, T.J.E., Caldwell, D.G., Ferrigno, G., De Momi, E., Mattos, L.S., Fiorini, P.: Design and integration of electrical bio-impedance sensing in surgical robotic tools for tissue identification and display. Frontiers in Robotics and AI **6**, 55 (2019)
3. Cheng, Z., Dall'Alba, D., Schwaner, K.L., Fiorini, P., Savarimuthu, T.R.: Robot assisted electrical impedance scanning for tissue bioimpedance spectroscopy measurement. Measurement **195**, 111112 (2022)
4. Cheng, Z., Savarimuthu, T.R.: Monopolar, bipolar, tripolar, and tetrapolar configurations in robot assisted electrical impedance sensing. Biomedical Physics & Engineering Express **8**(5), 055014 (2022)
5. Cheng, Z., Savarimuthu, T.R., Foong, S., Tan, U.X.: Design of adjustable constant force/torque mechanisms for medical applications. Journal of Mechanisms and Robotics **15**(2), 025001 (2023)
6. Dodde, R., Bull, J., Shih, A.: Bioimpedance of soft tissue under compression. Physiological measurement **33**(6), 1095 (2012)
7. Giannarou, S., Ye, M., Gras, G., Leibrandt, K., Marcus, H.J., Yang, G.Z.: Vision-based deformation recovery for intraoperative force estimation of tool–tissue interaction for neurosurgery. International journal of computer assisted radiology and surgery **11**(6), 929–936 (2016)
8. Giulianotti, P.C., Bianco, F.M., Daskalaki, D., Gonzalez-Ciccarelli, L.F., Kim, J., Benedetti, E.: Robotic liver surgery: technical aspects and review of the literature. Hepatobiliary surgery and nutrition **5**(4), 311 (2016)
9. Gonenc, B., Balicki, M.A., Handa, J., Gehlbach, P., Riviere, C.N., Taylor, R.H., Iordachita, I.: Preliminary evaluation of a micro-force sensing handheld robot for vitreoretinal surgery. In: 2012 IEEE/RSJ International Conference on Intelligent Robots and Systems. pp. 4125–4130. IEEE (2012)
10. Kim, U., Lee, D.H., Yoon, W.J., Hannaford, B., Choi, H.R.: Force sensor integrated surgical forceps for minimally invasive robotic surgery. IEEE Transactions on Robotics **31**(5), 1214–1224 (2015)
11. Kou, C.X., Dai, Y.H.: A modified self-scaling memoryless broyden–fletcher–goldfarb–shanno method for unconstrained optimization. Journal of Optimization Theory and Applications **165**(1), 209–224 (2015)
12. Marcus, H.J., Payne, C.J., Kailaya-Vasa, A., Griffiths, S., Clark, J., Yang, G.Z., Darzi, A., Nandi, D.: A "smart" force-limiting instrument for microsurgery: Laboratory and in vivo validation. PloS one **11**(9), e0162232 (2016)
13. Martinsen, O.G., Grimnes, S.: Bioimpedance and bioelectricity basics. Academic press (2011)
14. Payne, C.J., Latt, W.T., Yang, G.Z.: A new hand-held force-amplifying device for micromanipulation. In: 2012 IEEE International Conference on Robotics and Automation. pp. 1583–1588. IEEE (2012)
15. Rosen, J., Brown, J., De, S., Hannaford, B.: Macro and micro soft-tissue biomechanics and tissue damage: Application in surgical robotics. In: Surgical Robotics, pp. 583–618. Springer (2011)
16. Rosen, J., Brown, J.D., De, S., Sinanan, M., Hannaford, B.: Biomechanical properties of abdominal organs in vivo and postmortem under compression loads. Journal of biomechanical engineering **130**(2), 021020 (2008)
17. Semere, W., Kitagawa, M., Okamura, A.M.: Teleoperation with sensor/actuator asymmetry: Task performance with partial force feedback. In: 12th International Symposium on Haptic Interfaces for Virtual Environment and Teleoperator Systems, 2004. HAPTICS'04. Proceedings. pp. 121–127. IEEE (2004)